

# SCIENTIFIC REPORTS



OPEN

## Antioxidants inhibit advanced glycosylation end-product-induced apoptosis by downregulation of miR-223 in human adipose tissue-derived stem cells

Received: 14 September 2015

Accepted: 25 February 2016

Published: 11 March 2016

Zhe Wang<sup>1</sup>, Hongqiu Li<sup>2</sup>, Ran Guo<sup>3</sup>, Qiushi Wang<sup>1</sup> & Dianbao Zhang<sup>4</sup>

Advanced glycosylation end products (AGEs) are endogenous inflammatory mediators that induce apoptosis of mesenchymal stem cells. A potential mechanism includes increased generation of reactive oxygen species (ROS). MicroRNA-223 (miR-223) is implicated in the regulation of cell growth and apoptosis in several cell types. Here, we tested the hypothesis that antioxidants N-acetylcysteine (NAC) and ascorbic acid 2-phosphate (AAP) inhibit AGE-induced apoptosis via a microRNA-dependent mechanism in human adipose tissue-derived stem cells (ADSCs). Results showed that AGE-HSA enhanced apoptosis and caspase-3 activity in ADSCs. AGE-HSA also increased ROS generation and upregulated the expression of miR-223. Interestingly, reductions in ROS generation and apoptosis, and upregulation of miR-223 were found in ADSCs treated with antioxidants NAC and AAP. Furthermore, miR-223 mimics blocked antioxidant inhibition of AGE-induced apoptosis and ROS generation. Knockdown of miR-223 amplified the protective effects of antioxidants on apoptosis induced by AGE-HSA. miR-223 acted by targeting fibroblast growth factor receptor 2. These results indicate that NAC and AAP suppress AGE-HSA-induced apoptosis of ADSCs, possibly through downregulation of miR-223.

Human adipose tissue-derived stem cells (ADSCs) are multipotent stromal cells in adipose tissue. Emerging evidence has shown the beneficial effects of ADSC administration to treat various diseases<sup>1</sup>. Furthermore, ADSCs have been found to promote wound healing<sup>2</sup>. Diabetes is associated with an impaired ability to heal wounds. Accordingly, promotion of wound healing by stem cell therapy, which is observed in non-diabetic conditions, is significantly attenuated in diabetic patients<sup>3</sup>. Although autologous ADSC administration has been reported to improve healing in diabetic skin repair, impairment of resident and recruited stem cell functions strongly contributes to delays in wound healing under diabetic conditions<sup>4–6</sup>. However, approaches have not been developed to improve ADSC functions in diabetic individuals.

Previous studies have implicated advanced glycosylation end-products (AGEs) in impaired diabetic wound healing<sup>7</sup>. AGEs are a group of heterogeneous compounds formed by the Maillard reaction, which starts from stiff bases and the Amadori product,  $\alpha$  1-amino-1-deoxyketose, produced by the reaction of the carbonyl group of a reducing sugar. The Maillard reaction involves proteins via non-enzymatic glycation, lipids, and nucleic acids by reducing sugars and aldehydes. During Amadori reorganization, these highly reactive intermediate carbonyl groups, recognized as  $\alpha$ -dicarbonyls or oxoaldehydes, products of which induce 3-deoxyglucosone and methylglyoxal, tend to accumulate<sup>8</sup>. Recent studies indicate that AGE modification of proteins may lead to alterations of normal functions by inducing cross-linking of extracellular matrices. Intracellular formation of AGEs can also cause generalized cellular dysfunction. Furthermore, AGEs can mediate their effects via specific receptors,

<sup>1</sup>Department of Blood Transfusion, Shengjing Hospital of China Medical University, Shenyang 110004, China.

<sup>2</sup>Department of Orthopedics, Central Hospital of Shenyang Medical College, Shenyang 110024, China. <sup>3</sup>Department of Orthopaedics, Shengjing Hospital of China Medical University, Shenyang 110004, China. <sup>4</sup>Department of Stem Cells and Regenerative Medicine, Key Laboratory of Cell Biology, Ministry of Public Health, China medical University, Shenyang 110001, China. Correspondence and requests for materials should be addressed to Z.W. (email: wz\_cmu@126.com)

such as the receptor for AGE (RAGE), thus activating diverse signal transduction cascades and downstream pathways, including generation of reactive oxygen species (ROS). Oxidative stress occurs as a result of the imbalance between ROS production and antioxidant defenses. Sources of ROS include mitochondria, auto-oxidation of glucose, and enzymatic pathways, which include nicotinamide adenine dinucleotide phosphate reduced (NADPH) oxidase<sup>9,10</sup>. Apoptosis is a potential mechanism through which AGEs exert their effects on cellular dysfunction<sup>11,12</sup>. It has been shown that AGEs induce apoptosis in mesenchymal stem cells (MSCs) and endothelial progenitor cells (EPCs)<sup>13</sup>. Increases in MSC apoptosis contribute to delayed wound healing in diabetic rats<sup>14</sup>. Excessive production of ROS plays an important role in apoptosis<sup>15</sup>. It has been reported that AGEs induce MSC apoptosis through overproduction of intracellular ROS<sup>11</sup>.

L-Ascorbic acid 2-phosphate (AAP) is an oxidation-resistant derivative of ascorbic acid. It has been demonstrated that AAP promotes cell differentiation and DNA synthesis. N-acetyl-L-cysteine (NAC) is a prodrug/pre-cursor of the biological antioxidant glutathione. It is a potent ROS inhibitor and has been widely used to counter the adverse effects of oxidative stress<sup>16</sup>. However, the mechanism by which NAC and AAP protect cells from oxidative stress has not been fully elucidated. Recently, several microRNAs (miRNAs) have been found to interfere with and modulate intracellular apoptosis signaling<sup>17–20</sup>. In the current study, we employed NAC and AAP as antioxidants to reduce oxidative stress levels and apoptosis in ADSCs exposed to AGEs, and focused on how the protective effects are modulated by miRNAs for a potentially new therapeutic approach.

## Results

**Antioxidants suppress AGE-HSA-induced apoptosis and caspase-3 activity in ADSCs.** Cells were treated with HSA (300 µg/ml) or AGE-HSA (300 µg/ml) for 24 h. As shown in Fig. 1A, the cells treated with AGE-HSA showed an increase in apoptotic cell death compared with control cells. To determine whether antioxidants affect AGE-HSA-induced apoptosis and caspase-3 activity of ADSCs, the cells were pretreated with 3 mM NAC and 0.2 mM AAP for 20 h and then treated with AGE-HSA (300 µg/ml) for 24 h. The levels of apoptosis and caspase-3 activity of ADSCs were then determined by enzyme-linked immunosorbent assays (ELISAs). We found that the antioxidants significantly suppressed AGE-HSA-induced apoptosis ( $P < 0.05$ ) (Fig. 1A). Caspase-3 is the principal effector caspase through which the mitochondrial and cytosolic pathways induce apoptosis. Therefore, we measured the levels of caspase-3 activity in each group (Fig. 1B). AGE-HSA significantly increased caspase-3 activity in treated cells compared with control cells ( $P < 0.05$ ). Interestingly, antioxidants significantly suppressed the AGE-HSA-induced caspase-3 activity of ADSCs ( $P < 0.05$ ).

**Antioxidants suppress oxidative stress levels in ADSCs induced by AGE-HSA.** The effects of AGEs on apoptosis of ADSCs are mediated by production of ROS. To determine whether antioxidants affect ROS production, the cells were pretreated with 3 mM NAC and 0.2 mM AAP for 20 h and then treated with AGE-HSA (300 µg/ml) for 24 h. Production of ROS was then determined by DCFH-DA. As shown in Fig. 1C,D, the antioxidants significantly suppressed ROS production in ADSCs induced by AGE-HSA ( $P < 0.05$ ).

**Antioxidants suppress upregulation of miR-223 in ADSCs induced by AGE-HSA.** MiR-223 has been found to interfere with and modulate intracellular apoptosis signaling. To determine whether AGE-HSA affects the expression of miR-223 in ADSCs, the cells were treated with HSA (300 µg/ml) or AGE-HSA (50–500 µg/ml) for 24 h, and then the expression of miR-223 was determined by RT-PCR. As shown in Fig. 2A, cells treated with AGE-HSA showed an increase in the expression of miR-223. To determine whether antioxidants affect the expression of miR-223 in ADSCs induced by AGE-HSA, the cells were pretreated with antioxidants for 20 h and then treated with AGE-HSA (300 µg/ml) for 24 h. Expression of miR-223 was then determined by RT-PCR. As shown in Fig. 2B, antioxidant pretreatment significantly suppressed upregulation of miR-223 in ADSCs induced by AGE-HSA ( $P < 0.05$ ).

**Role of miR-223 in the protective effects of antioxidants against AGE-HSA-induced apoptosis, caspase-3 activity, and oxidative stress levels in ADSCs.** To assess the role of miR-223 in response to AGE-HSA and antioxidant treatments, apoptosis and ROS generation were examined in ADSCs in the presence or absence of miR-223 mimics or inhibitors. MiR-223 expression was confirmed by RT-PCR. The results of apoptosis analysis showed that transfection of miR-223 mimics positively regulated the apoptosis induced by AGE-HSA ( $P < 0.05$ ) (Fig. 3A). Moreover, the results of caspase-3 activity analysis showed that transfection of miR-223 mimics positively regulated the caspase 3 activity induced by AGE-HSA ( $P < 0.05$ ) (Fig. 3B). Measurement of cellular ROS generation showed that transfection of miR-223 mimics positively regulated the ROS generation induced by AGE-HSA ( $P < 0.05$ ) (Fig. 3C,D). In contrast, cells transfected with miR-223 inhibitors showed negative regulation of the apoptosis induced by AGE-HSA ( $P < 0.05$ ) (Fig. 4A). Furthermore, transfection of miR-223 inhibitors negatively regulated the caspase 3 activity induced by AGE-HSA ( $P < 0.05$ ) (Fig. 4B). Transfection of miR-223 inhibitors also resulted in negative regulation of the ROS generation induced by AGE-HSA ( $P < 0.05$ ) (Fig. 4C,D). To further examine whether miR-223 was required for the protective effects of antioxidants against apoptosis induced by AGE-HSA, cells were transfected with miR-223 mimics or inhibitors in the presence or absence of antioxidants and then treated with AGE-HSA (300 µg/ml) for 24 h. We found that the protection conferred by the antioxidants was diminished by upregulation of miR-223, but amplified by downregulation of miR-223 (Figs 3 and 4). These results indicated that miR-223 may act as a positive modulator of AGE-HSA-induced apoptosis in ADSCs, and that antioxidants inhibit AGE-HSA-induced apoptosis by downregulation of miR-223 in ADSCs.

**FGFR2 is a direct target of miR-223.** Next, we identified the miR-223 target gene to gain a further insight into the molecular mechanisms of miR-223 in the protective effects of antioxidants against AGE-HSA-induced apoptosis. The public database-TargetScan (<http://www.targetscan.org>) was used to predict the potential target of

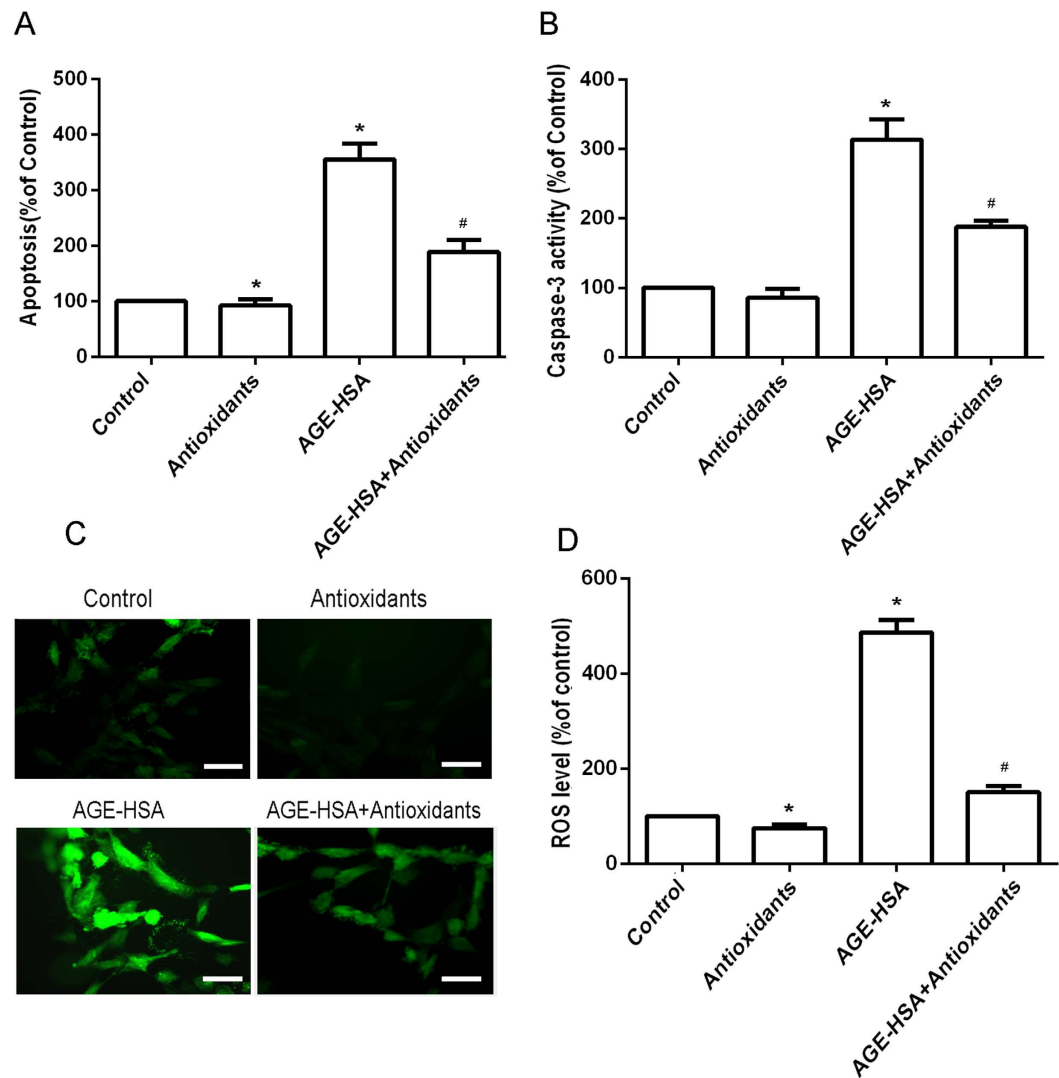


**Figure 1. Effects of antioxidants on AGE-HSA-induced apoptosis, caspase-3 activity, and ROS generation in ADSCs.** Cells were pretreated with antioxidants followed by treatment with AGE-HSA (300  $\mu\text{g/ml}$ ) for 24 h. The level of apoptosis (A) and caspase-3 activity (B) were measured by ELISA. (C) Intracellular ROS generation was visualized under the fluorescence microscope. The scale bars represent 100  $\mu\text{m}$ . (D) The level of DCF-sensitive ROS was measured by a flow cytometer. Each value is expressed as the mean  $\pm$  SD of three independent experiments. \* $P < 0.05$  vs. control (HSA 300  $\mu\text{g/ml}$ ). # $P < 0.05$  vs. AGE-HSA-treated group (300  $\mu\text{g/ml}$ ).

miR-223. Because of a critically conserved binding site, *FGFR2* was selected for further examination (Fig. 5A). To confirm that *FGFR2* is a direct target of miR-223, we constructed the luciferase reporter pGL3-*FGFR2*-3'-UTR. Scrambled target sites (pGL3-*FGFR2*-MUT) were used as controls for sequence specificity. The luciferase activity of the pGL3-*FGFR2*-30-UTR reporter was significantly suppressed in miR-223-transfected ADSCs compared with Negative Control (NC)-transfected cells normalized to a control vector containing Renilla luciferase, pRL-TK. In contrast, there was no significant difference in the relative luciferase activity of the pGL3-fibroblast-like growth factor receptor 2 (*FGFR2*)-MUT reporter in miR-223-transfected ADSCs compared with NC-transfected cells ( $P > 0.05$ ) (Fig. 5B). These results showed that *FGFR2* underwent direct negative regulation by miR-223 in ADSCs. In support of these results, we examined *FGFR2* protein and mRNA levels in miR-223- or anti-miR-223-transfected cells, and their respective NC and parental cells by RT-PCR and western blotting, respectively. We observed a clear reduction in the level of endogenous *FGFR2* protein in miR-223-transfected cells compared with NC-transfected and parental cells normalized to an endogenous reference, GAPDH (Fig. 5D). Overexpression of *IGFR* protein was also found in anti-miR-223-transfected cells compared with anti-NC-transfected and parental cells (Fig. 5F). These results demonstrated that miR-223 may target *FGFR2* in ADSCs. Despite the effect of miR-223 on *FGFR2* protein levels, no effect on *FGFR2* mRNA levels was detected (Fig. 5C).

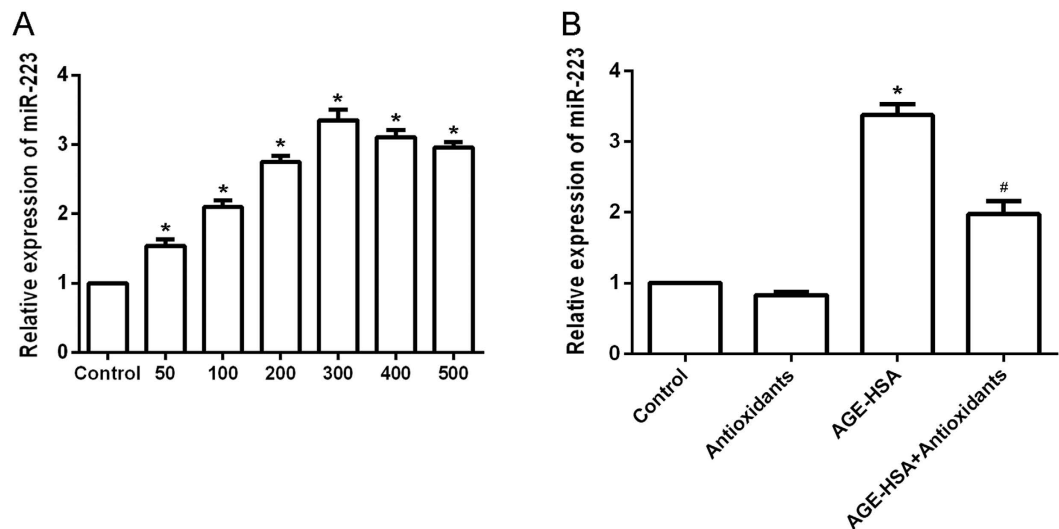


**Figure 2. Effects of antioxidants on AGE-HSA-induced upregulation of miR-223 in ADSCs.** (A) Cells were incubated with HSA (300 µg/ml) or AGE-HSA (50–500 µg/ml) for 24 h. (B) Cells were pretreated with antioxidants followed by treatment with AGE-HSA (300 µg/ml) for 24 h. The mRNA expression level of miR-223 was analyzed by RT-PCR. Each value is expressed as the mean  $\pm$  SD of three independent experiments. \* $P < 0.05$  vs. control (300 µg/ml HSA). # $P < 0.05$  vs. AGE-HSA-treated group (300 µg/ml).

**FGFR2 is involved in the protective effect of antioxidants on AGE-HSA-induced apoptosis.** Next, we further examined whether the counteraction of miR-223 overexpression against the protective effect of antioxidants on AGE-HSA-induced apoptosis is mediated by FGFR2. The expression of FGFR2 in cells treated with 300 µg/ml AGE-HSA for 24 h after pretreatment with antioxidants for 20 h was analyzed by western blotting. In addition, the apoptosis and ROS production of FGFR2 knockdown ADSCs stimulated with AGE-HSA for 24 h after pretreatment with antioxidants for 20 h were assessed. FGFR2 expression in cells was decreased following AGE-HSA treatment for 24 h ( $P < 0.05$ ) (Fig. 6A), and antioxidant pretreatment for 20 h restored the expression of FGFR2 in ADSCs treated with AGE-HSA (Fig. 6B). Knockdown of FGFR2 clearly diminished the protective effect of antioxidants on AGE-HSA-induced apoptosis in ADSCs ( $P < 0.05$ ) (Fig. 6D–G). The results revealed that overexpression of FGFR2 could argue the protective effect of antioxidants on AGE-HSA-induced apoptosis in ADSCs (Fig. 7). These data indicated that FGFR2 was involved in the protective effect of antioxidants on AGE-HSA-induced apoptosis in ADSCs.

## Discussion

Despite the fact that recent preclinical studies have shown beneficial effects of ADSC administration for treating a wide variety of diseases, including animal models of diabetes<sup>5,21–23</sup>, impairment of resident and recruited cell functions strongly contributes to delays in wound healing under diabetic conditions. A number of studies have suggested that diabetes mediates stem cell apoptosis and plays an important role in the pathogenesis of biophysical disorders<sup>24,25</sup>. However, the mechanism of diabetes in the impairment of ADSC functions and approaches has been not elucidated.

AGEs are noxious metabolic products that have been found to significantly accumulate in diabetic patients in comparison with normal individuals. They cause adverse effects on the growth of several cell types such as vascular endothelial cells and renal tubular epithelial cells. The elevated levels of AGEs in diabetic patients induce pathological changes such as promotion of EPC and endothelial cell apoptosis<sup>26</sup>. Our previous study confirmed that AGEs promote apoptosis of ADSCs *in vitro* via a receptor for the advanced glycation end-product (RAGE)-dependent p38 MAPK pathway<sup>7</sup>. The interaction of AGEs with RAGE regulates various cellular processes and leads to increased production of ROS. In this study, as expected, we found a significant increase in the production of ROS in AGE-HSA-treated cells compared with that in the control. Excessive production of ROS due to sustained oxidative stress in diabetic patients affects the survival of engrafted MSCs. The increase in ROS might damage proteins, DNA, and lipids of engrafted cells. In addition, increased ROS production induces superoxide in the cell membrane and damages cell membrane proteins, resulting in calcium influx and ultimately an abnormal cell structure, functions, and metabolic activity, as well as mitochondrial dysfunction or apoptosis<sup>16</sup>. Furthermore, as a second messenger, ROS stimulates important signal transduction pathways, regulates cell functions, and triggers signaling cascades, such as mitogen-activated protein kinase and NF- $\kappa$ B, which regulate gene expression and induce cell apoptosis<sup>27,28</sup>.

Co-treatment with NAC and AAP to prevent cell death and injury due to oxidative stress is largely based on *in vitro* observations. Turgeon *et al.* reported that probucol and antioxidant vitamins rescue ischemia-induced neovascularization in mice exposed to cigarette smoke by improving the functions of EPCs. Previous reports have also shown that addition of other antioxidants, such as epigallocatechin-3-gallate, curcumin, melatonin, and b-estradiol, reduce cellular oxidative stress and inhibit the apoptosis of MSCs<sup>4</sup>. In this study, we first identified

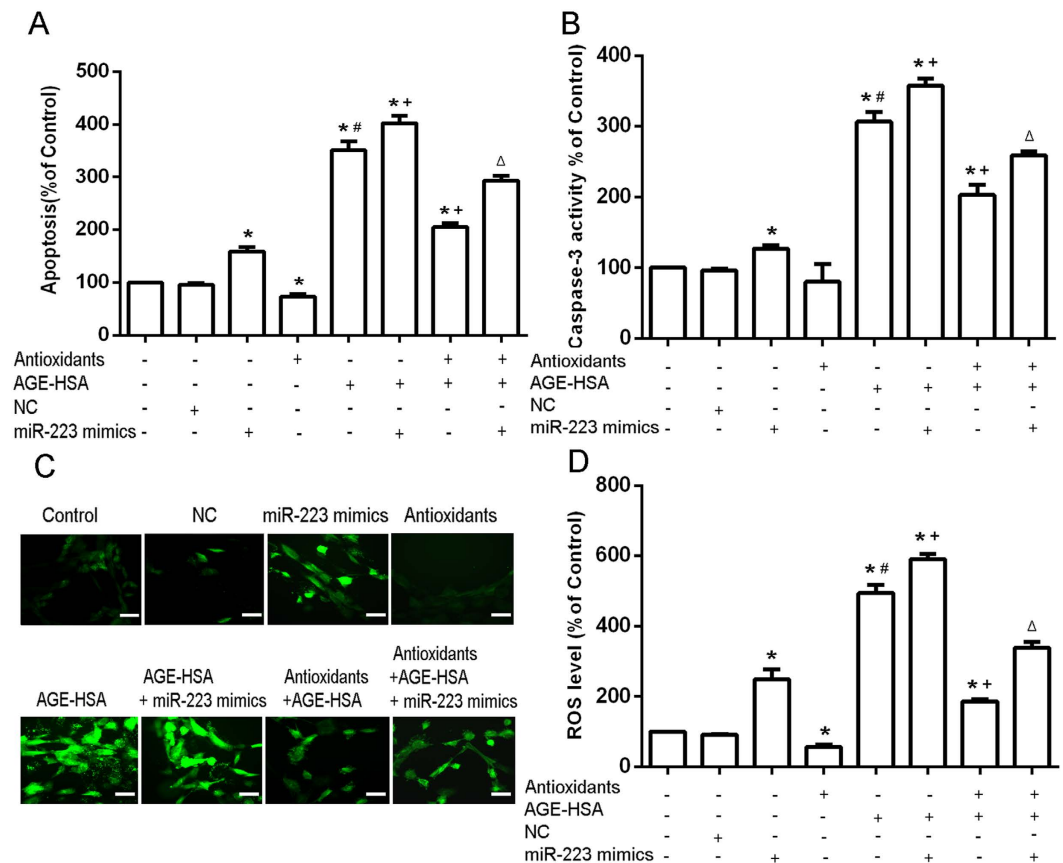


**Figure 3. Role of overexpression of miR-223 in the protective effects of antioxidants on AGE-HSA-induced apoptosis of ADSCs.** Cells were transfected with miR-223 mimics and/or pretreated with antioxidants and subsequently treated with AGE-HSA (300  $\mu$ g/ml) for 24 h. The levels of apoptosis (A) and caspase-3 activity (B) were measured by ELISA. (C) Intracellular ROS generation was visualized under the fluorescence microscope. The scale bars represent 100  $\mu$ m. (D) The level of DCF-sensitive ROS was measured by a flow cytometer. Each value is expressed as the mean  $\pm$  SD of three independent experiments. \*P < 0.05 vs. control (HSA 300  $\mu$ g/ml), #P < 0.05 vs. antioxidant pretreatment (3 mM NAC and 0.2 mM AAP), +P < 0.05 vs. AGE-HSA (300  $\mu$ g/ml),  $\Delta$ P < 0.05 vs. antioxidant pretreatment (3 mM NAC and 0.2 mM AAP) and AGE-HSA (300  $\mu$ g/ml).

the optimal combination of NAC and AAP (3 mM and 0.2 mM, respectively) to exert protective effects on ADSCs under AGE-HSA-induced oxidative stress. Based on these data, we hypothesized that antioxidants suppressed AGE-HSA-induced apoptosis in ADSCs. Under ROS production induced by treatment with 300  $\mu$ g/l AGE-HSA for 24 h, we found significant decreases in the levels of apoptosis and caspase-3 activity when cells were pretreated with NAC and AAP for 20 h. These results are consistent with a report by Li *et al.* who found synergistic protection conferred by NAC and AAP against mitoptosis, necroptosis, and apoptosis in human MSCs treated with H<sub>2</sub>O<sub>2</sub>. Our data indicate that a reduction in oxidative stress levels by antioxidants might represent a novel therapeutic strategy to improve the survival of ADSCs exposed to AGEs.

Several recent reports have indicated the involvement of miRNAs in the regulation of intracellular ROS production and apoptosis signaling during diabetes<sup>29,30</sup>. Additionally, elevated expression of miR-21 mediates the oxidative stress response by increasing intracellular ROS levels and impairing nitric oxide bioavailability via targeting human superoxide dismutase-2<sup>31</sup>. ROS production and apoptosis of AGE-treated endothelial cells involves suppression of miR-200b/miR-200c by upregulation of RhoA/ROCK2 signaling<sup>32</sup>. Apoptosis of human umbilical vein endothelial cells exposed to AGEs also involves miR-223 via targeting IGFR1<sup>33</sup>. Here, we aimed to clarify the biological role of miR-223 in ADSC apoptosis regulation by AGE-HSA and antioxidants. The results showed a significant increase in the miR-223 expression of ADSCs treated with AGE-HSA, but a reduction of in miR-223 expression when cells were pretreated with antioxidants before treatment with AGE-HSA. Reintroduction of miR-223 by transient transfection or siRNA silencing of the target gene (FGFR2) blocked the protective effects of antioxidants on AGE-HSA-induced apoptosis and increased the production of ROS, while increasing the level of apoptosis and activity of caspase-3 in ADSCs. Our results support the notion that protective effects of antioxidants on AGE-HSA-induced apoptosis in ADSCs are partially mediated by a reduction in miR-223 expression.

In conclusion, the present study suggests that miR-223 transfection bypasses antioxidant suppression of AGE-induced apoptosis at least partially through upregulation of FGFR2 expression. Downregulation of miR-223, through its positive effects on ADSCs, might help to restore the ability to heal wounds in diabetic individuals.



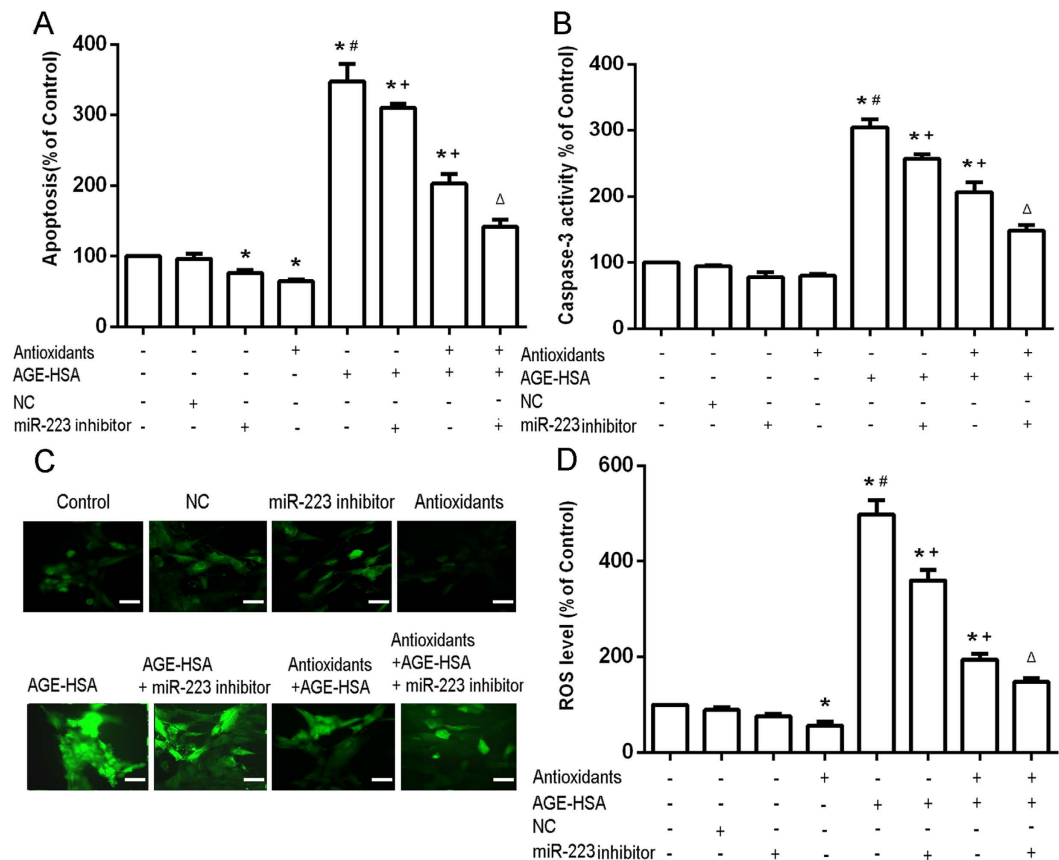


**Figure 4. Role of downregulation of miR-223 in the protective effects of antioxidants on AGE-HSA-induced apoptosis of ADSCs.** Cells were transfected with miR-223 inhibitors and/or pretreated with antioxidants and subsequently treated with AGE-HSA (300  $\mu$ g/ml) for 24 h. The levels of apoptosis (A) and caspase-3 activity (B) were measured by ELISA. (C) Intracellular ROS generation was visualized under the fluorescence microscope. The scale bars represent 100  $\mu$ m. (D) The level of DCF-sensitive ROS was measured by a flow cytometer. Each value is expressed as the mean  $\pm$  SD of three independent experiments. \* $P < 0.05$  vs. control (HSA 300  $\mu$ g/ml), # $P < 0.05$  vs. antioxidant pretreatment (3 mM NAC and 0.2 mM AAP), + $P < 0.05$  vs. AGE-HSA (300  $\mu$ g/ml),  $\Delta P < 0.05$  vs. antioxidant pretreatment (3 mM NAC and 0.2 mM AAP) and AGE-HSA (300  $\mu$ g/ml).

Whether similar effects can be obtained in other clinical situations involving increased oxidative stress levels such as atherosclerotic diseases and hypercholesterolemia remains to be determined. If this is the case, modification of oxidative stress levels by miRNAs might represent a novel therapeutic strategy to restore impaired cell functions and promote wound healing by ADSCs exposed to AGEs.

## Materials and Methods

**Cell culture and treatments.** All the methods were carried out in accordance with the approved guidelines and all experimental protocols were approved by the ethics committee of China Medical University. Adipose tissue samples were obtained with informed consent from 10 patients at the Shengjing Hospital of China Medical University. Cells were isolated and harvested as described previously<sup>7</sup>. ADSC identities were confirmed by cell surface markers. For NAC and AAP (both purchased from Sigma Co., MO, USA) co-treatment, ADSCs were pretreated with 3 mM NAC and 0.2 mM AAP for 20 h, followed by incubation in medium containing 300  $\mu$ g/ml AGE-HSA (Sigma) for 24 h.

**Transfection of miRNA mimics and inhibitors, siRNAs, and pReceiver FGFR2.** Cells ( $5 \times 10^5$ ) were seeded in a 6-well plate (Nest Biotechnology, Hong Kong, China). At 70% confluence, the cells were transfected with miR-223 mimics, miR-223 inhibitors, or a negative control. After 20 h, the cells were treated with or without 300  $\mu$ g/ml AGE-HSA. Transfection of miR-223 mimics or inhibitors was carried out as described previously<sup>11</sup>. Analyses were performed at 24 h after transfection. siRNAs targeting fibroblast growth factor receptor 2 (FGFR2) and a control (scramble siRNA) were purchased from Santa Cruz Biotechnology. Transfection of 50 nM siRNA or scramble siRNA was performed as described previously. The human FGFR2-coding sequence excluding the 3'-UTR was inserted into a pReceiver vector (Genecopoeia, USA) to construct the pReceiver-FGFR2 vector. The cells were transfected with pReceiver FGFR2 or an empty pReceiver vector. All results are representative of three independent experiments.

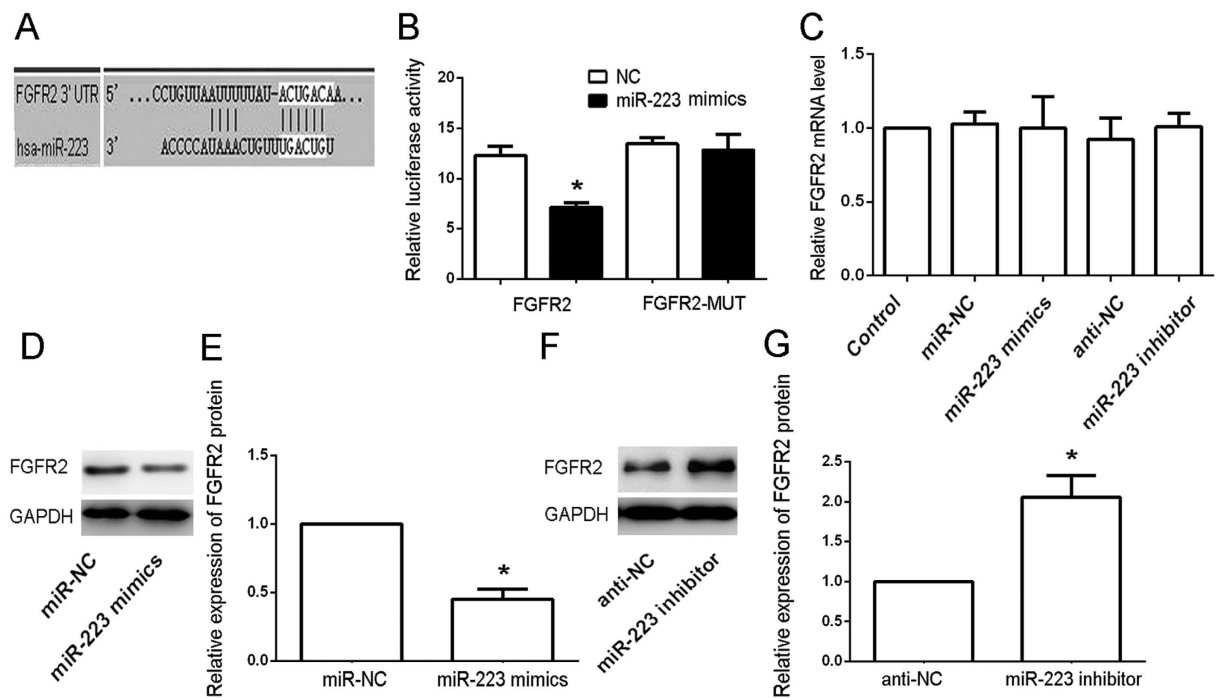


**Figure 5. FGFR2 is a direct target of miR-223 in ADSCs.** (A) miR-223 directly targeted FGFR2. (B) Analysis of the luciferase activities of FGFR2 and FGFR2-MUT in ADSCs transfected with miR-223 mimics or NCs. \* $P < 0.05$ . (C) mRNA expression analysis of FGFR2 in parental and transfected cells by RT-PCR. No significant difference in the levels of endogenous FGFR2 mRNA was found in transfected and parental cells normalized to an endogenous reference (GAPDH). (D,E) Protein expression analysis of FGFR2 in miR-223 mimic-transfected, NC-transfected, and parental cells by western blotting. A clear reduction in the level of endogenous FGFR2 protein was found in miR-223 mimic-transfected cells compared with NC-transfected cells normalized to an endogenous reference (GAPDH). (F,G) Protein expression analysis of FGFR2 in miR-223 inhibitor-transfected, NC-transfected, and parental cells by western blotting. A clear increase in the level of endogenous FGFR2 protein was found in miR-223 mimic-transfected cells compared with NC-transfected cells normalized to an endogenous reference (GAPDH).

**Apoptosis assay.** For apoptosis assays, cells were seeded in 96-well plates at a density of  $2 \times 10^4$  cells per well. At approximately 80% confluence, the cells were cultured in high glucose DMEM medium (GIBCO, Gaithersburg, MD, USA) supplemented with 10% fetal bovine serum (FBS, GIBCO, Gaithersburg, MD, USA). To induce apoptosis, ADSCs were exposed to AGE-HSA (300  $\mu\text{g}/\text{ml}$ ) for 24 h. To determine the role of antioxidants in apoptosis, ADSCs were pretreated with 3 mM NAC and 0.2 mM AAP for 20 h, and then apoptosis was induced by treatment with 300  $\mu\text{g}/\text{ml}$  AGE-HSA for 24 h. The level of apoptosis was determined using the Cell Death Detection ELISAPLUS kit (Roche Applied Science, Indianapolis, IN, USA), which detects cytoplasmic histone-associated DNA fragments, according to the manufacturer's instructions.

**Caspase-3 activity assay.** As a marker of apoptosis, caspase-3 activation was assessed using the Caspase-Glo3/7 Assay (Promega, Madison, USA) according to the manufacturer's instructions.

**Measurement of intracellular ROS.** Intracellular ROS and  $\text{O}_2$  generation were assessed using 2',7'-dichlorofluorescein diacetate (DCFH-DA, Sigma) as described previously<sup>34</sup>. Briefly, ADSCs grown in 10-cm plates were subjected to the various culture conditions described above. The medium was replaced with control medium containing 10  $\mu\text{M}$  DCFH-DA, and the cells were incubated for 30 min in the dark. Intracellular ROS generation was then visualized under a fluorescence microscope (Olympus, Tokyo, Japan). DCF fluorescence was measured by a flow cytometer. Data were normalized to the control values.

**RNA extraction and reverse transcription-polymerase chain reaction (RT-PCR).** RT-PCR was performed as described previously<sup>35</sup>. Briefly, total RNA was extracted from each sample using Trizol reagent (Invitrogen, CA, USA) according to the manufacturer's instructions. The quality of the isolated RNA was checked by agarose gel electrophoresis. RNA concentrations were determined by measuring the optical density at 260 and 280 nm. To analyze miR-223 expression, RT-PCR was performed using specific stem-loop RT primers from a Hairpin-in miRNA qPCR Quantitation Kit (GenePharma, Shanghai, China). Quantitative real-time PCR was performed using the same kit on the Applied Biosystems 7500 system. U6 was used as an internal control. To analyze FGFR2 mRNA expression, cDNA synthesis was carried out using random hexamer primers and MMLV reverse transcriptase under the conditions recommended by the manufacturer (Invitrogen). Specific primers were

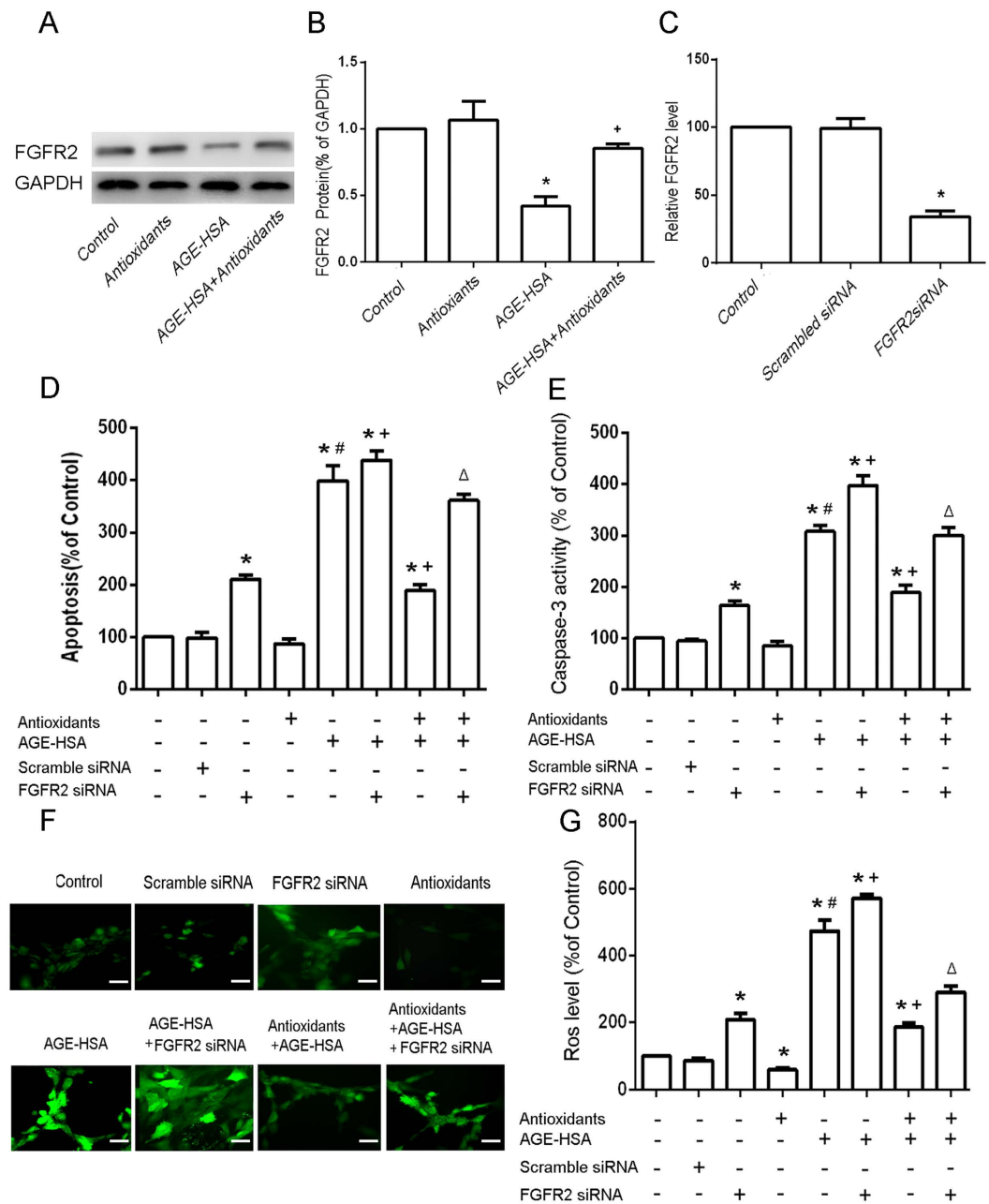


**Figure 6. Effects of siFGFR2 on the protective effects of antioxidants against AGE-HSA-induced apoptosis in ADSCs.** (A) Cells were pretreated with antioxidants followed by treatment with AGE-HSA (300  $\mu$ g/ml) for 24 h. The protein expression level of FGFR2 was analyzed by western blotting. (B) Results from three independent western blots were quantified by ImageJ software. (C) FGFR2 silencing was verified by RT-PCR. FGFR2 siRNA-transfected ADSCs were pretreated with antioxidants followed by treatment with AGE-HSA (300  $\mu$ g/ml) for 24 h. The levels of apoptosis (D) and caspase-3 activity (E) were measured by ELISA. (F) Intracellular ROS generation was visualized under the fluorescence microscope. The scale bars represent 100  $\mu$ m. (G) The level of DCF-sensitive ROS was measured by a flow cytometer. Each value is expressed as the mean  $\pm$  SD of three independent experiments. \* $P < 0.05$  vs. control (HSA 300  $\mu$ g/ml), # $P < 0.05$  vs. antioxidants (3 mM NAC and 0.2 mM AAP), + $P < 0.05$  vs. AGE-HSA (300  $\mu$ g/ml),  $\Delta P < 0.05$  vs. antioxidants (3 mM NAC and 0.2 mM AAP) and AGE-HSA (300  $\mu$ g/ml).

designed using Gene Runner software (Hastings Software, Inc.). Glyceraldehyde-3-phosphate dehydrogenase (GAPDH) was used as an internal control. Fold changes of both miRNA and mRNA expression were calculated using the  $2^{-\Delta\Delta C_t}$  method. Primer sequences and PCR conditions are shown in Table 1.

**Dual luciferase reporter assay.** A dual luciferase reporter assay was performed as reported previously<sup>36</sup>. Briefly, cells were seeded in 96-well plates and co-transfected with the pMir-Report luciferase vector, pRL-TK



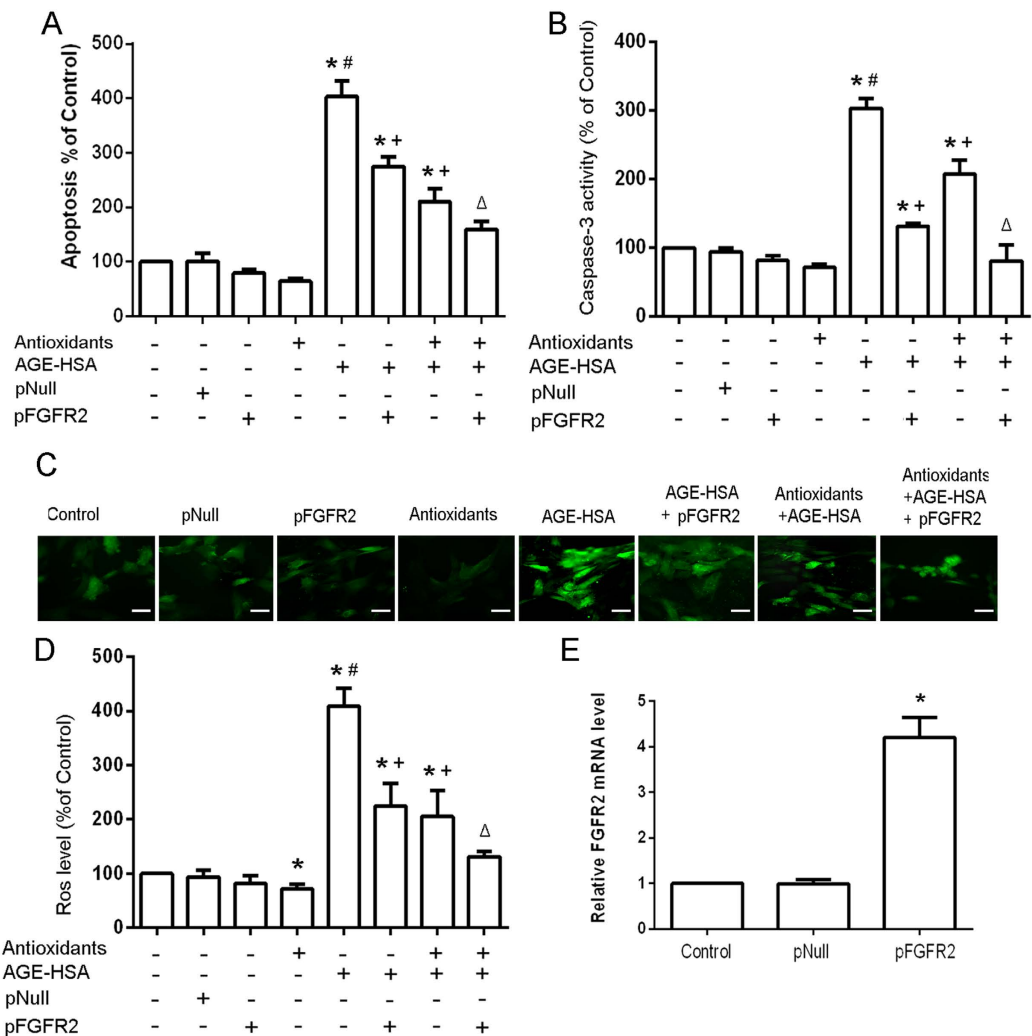


**Figure 7. Effects of restoring FGFR2 on the protective effects of antioxidants against AGE-HSA-induced apoptosis in ADSCs.** The levels of apoptosis (A) and caspase-3 activity (B) were measured by ELISA. (C) Intracellular ROS generation was visualized under the fluorescence microscope. The scale bars represent 100  $\mu$ m. (D) The level of DCF-sensitive ROS was measured by a flow cytometer. (E) Forced expression of FGFR2 was verified by RT-PCR. pReceiver-E2F3 or an empty pReceiver vector-transfected ADSCs were pretreated with antioxidants followed by treatment with AGE-HSA (300  $\mu$ g/ml) for 24 h. Each value is expressed as the mean  $\pm$  SD of three independent experiments. \* $P < 0.05$  vs. control (HSA 300  $\mu$ g/ml), # $P < 0.05$  vs. antioxidants (3 mM NAC and 0.2 mM AAP), + $P < 0.05$  vs. AGE-HSA (300  $\mu$ g/ml),  $\Delta P < 0.05$  vs. antioxidants (3 mM NAC and 0.2 mM AAP) and AGE-HSA (300  $\mu$ g/ml).

|       | Primer sequence                 | Product size (bp) | Ta ( $^{\circ}$ C)/cycles |
|-------|---------------------------------|-------------------|---------------------------|
| FGFR2 | S: 5'-GGTGGCTGAAAAACGGGAAG-3'   | 104               | 60.5/38                   |
|       | AS: 5'-AGATGGGACCACACTTCCATA-3' |                   |                           |
| GAPDH | S: 5'-ACCACAGTCCATGCCATCAC-3'   | 452               | 56.0/26                   |
|       | AS: 5'-TCCACCACCCTGTTGCTGTA-3'  |                   |                           |

**Table 1. Sequences of primers and PCR conditions.** S, sense; AS, antisense; Ta, annealing temperature.

Renilla luciferase vector, and miR-223 mimics as reported previously. After 48 h, the luciferase activities were determined with the Dual Luciferase Reporter Assay System (Promega). All results are representative of three independent experiments.

**Western blot analysis.** Proteins were isolated from harvested cells by mechanical disruption and the Mammalian Cell Lysis Kit (Sigma) according to the manufacturer's instruction. The proteins were separated on 1-mm NuPage Novex 10% Bis-Tris gels using the NuPage MOPS SDS Buffer Kit (Life Technologies, Carlsbad,

CA, USA) followed by electrotransfer to 0.2-mm nitrocellulose membranes (Pall, Port Washington, WI, USA). Nonspecific binding sites were blocked with 5% bovine serum albumin in PBS for 1 h at room temperature. The membranes were then incubated with diluted FGFR2 (1:1000; Cell Signaling Technology, Inc.) at 4°C overnight. After three washes with PBS containing 0.5% Tween-20, the membranes were incubated with a diluted horseradish peroxidase-conjugated secondary anti-rabbit (GE Healthcare, Buckinghamshire, UK) at room temperature for 2 h. The signal was visualized with enhanced chemiluminescent reagent (Amersham Biosciences, Piscataway, NJ, USA). As a protein loading control, blots were stripped and stained for GAPDH using an anti-GAPDH antibody (1:2000, AbCam, Cambridge, MA, USA).

**Statistical Analysis.** Statistical analysis was performed using SPSS version 19.0 software. Data are presented as the means  $\pm$  standard deviation (SD). Univariate comparisons of the means were performed using the Student's t-test with a significance threshold of  $P < 0.05$ . The data shown in figures are representative of three independent experiments.

## References

- Minteer, D. M., Marra, K. G. & Rubin, J. P. Adipose stem cells: biology, safety, regulation, and regenerative potential. *Clin Plast Surg.* **42**, 169–179 (2015).
- Jiang, D. *et al.* The effect of adipose tissue derived MSCs delivered by a chemically defined carrier on full-thickness cutaneous wound healing. *Biomaterials.* **34**, 2501–2515 (2013).
- El-Ftesi, S., Chang, E. I., Longaker, M. T. & Gurtner, G. C. Aging and diabetes impair the neovascular potential of adipose-derived stromal cells. *Plast Reconstr Surg.* **123**, 475–485 (2009).
- Dzhoyashvili, N. A. *et al.* Disturbed angiogenic activity of adipose-derived stromal cells obtained from patients with coronary artery disease and diabetes mellitus type 2. *J Transl Med.* **12**, 337 (2014).
- Cianfarani, F. *et al.* Diabetes impairs adipose tissue-derived stem cell function and efficiency in promoting wound healing. *Wound Repair Regen.* **21**, 545–553 (2013).
- Koči, Z. *et al.* Characterization of human adipose tissue-derived stromal cells isolated from diabetic patient's distal limbs with critical ischemia. *Cell Biochem Funct.* **32**, 597–604 (2014).
- Wang, Z. *et al.* Effect of advanced glycosylation end products on apoptosis in human adipose tissue-derived stem cells *in vitro*. *Cell Biosci.* **5**, 3 (2015).
- Goldin, A., Beckman, J. A., Schmidt, A. M. & Creager, M. A. Advanced glycation end products: sparking the development of diabetic vascular injury. *Circulation.* **114**, 597–605 (2006).
- Tan, A. L., Forbes, J. M. & Cooper, M. E. AGE, RAGE, and ROS in diabetic nephropathy. *Semin Nephrol.* **27**, 130–143 (2007).
- Ahmed, N. Advanced glycation endproducts-role in pathology of diabetic complications. *Diabetes Res Clin Pract.* **67**, 3–21 (2005).
- Nowotny, K., Jung, T., Höhn, A., Weber, D. & Grune, T. Advanced Glycation End Products and Oxidative Stress in Type 2 Diabetes Mellitus. *Biomolecules.* **5**, 194–222 (2015).
- Yamagishi, S. *et al.* Advanced Glycation End Products-Induced Apoptosis and Overexpression of Vascular Endothelial Growth Factor in Bovine Retinal Pericytes. *Biochem Biophys Res Commun.* **290**, 973–978 (2002).
- Weinberg, E., Maymon, T. & Weinreb, M. AGEs induce caspase-mediated apoptosis of rat BMSCs via TNF $\alpha$  production and oxidative stress. *J Mol Endocrinol.* **52**, 67–76 (2014).
- Kume, S. *et al.* Advanced glycation end-products attenuate human mesenchymal stem cells and prevent cognate differentiation into adipose tissue, cartilage, and bone. *J Bone Miner Res.* **20**, 1647–1658 (2005).
- Ullah, I., Park, H. Y. & Kim, M. O. Anthocyanins protect against kainic acid-induced excitotoxicity and apoptosis via ROS-activated AMPK pathway in hippocampal neurons. *CNS Neurosci Ther.* **20**, 327–338 (2014).
- Li, C. J., Sun, L. Y. & Pang, C. Y. Synergistic Protection of N-Acetylcysteine and Ascorbic Acid 2-Phosphate on Human Mesenchymal Stem cells Against Mitoptosis, Necroptosis and Apoptosis. *Sci Rep.* **24**, 9819 (2015).
- Byrom, M. W. & Cheng, A. M. Antisense inhibition of human miRNAs and indications for an involvement of miRNA in cell growth and apoptosis. *Nucleic Acids Res.* **33**, 1290–1297 (2005).
- Shang, Y., Wang, L. Q., Guo, Q. Y. & Shi, T. L. MicroRNA-196a overexpression promotes cell proliferation and inhibits cell apoptosis through PTEN/Akt/FOXO1 pathway. *Int J Clin Exp Pathol.* **8**, 2461–2472 (2015).
- Su, Z., Yang, Z., Xu, Y., Chen, Y. & Yu, Q. MicroRNAs in apoptosis, autophagy and necroptosis. *Oncotarget.* **206**, 8474–8490 (2015).
- Nie, Y. *et al.* Identification of MicroRNAs involved in hypoxia- and serum deprivation-induced apoptosis in mesenchymal stem cells. *Int J Biol Sci.* **7**, 762–768 (2011).
- Locke, M., Feisst, V. & Dunbar, P. Human adipose-derived stem cells: separating promise from clinical need. *Stem Cells.* **29**, 404–411 (2011).
- Jin, H. J. *et al.* Comparative analysis of human mesenchymal stem cells from bone marrow, adipose tissue, and umbilical cord blood as sources of cell therapy. *Int J Mol Sci.* **14**, 17986–18001 (2013).
- Al-Nbaheen, M. *et al.* Human stromal (mesenchymal) stem cells from bone marrow, adipose tissue and skin exhibit differences in molecular phenotype and differentiation potential. *Stem Cell Rev Rep.* **9**, 32–43 (2013).
- Publishing, S. The influence of diabetes enhanced inflammation on cell apoptosis and periodontitis. *Adv Biosci Biotechnol.* **3**, 712–719 (2012).
- Mabed, M. & Shahin, M. Mesenchymal stem cell-based therapy for the treatment of type 1 diabetes mellitus. *Curr Stem Cell Res Ther.* **7**, 179–90 (2012).
- Li, B. *et al.* Induction of lactadherin mediates the apoptosis of endothelial cells in response to advanced glycation end products and protective effects of grape seed procyanidin B2 and resveratrol. *Apoptosis.* **16**, 732–745 (2012).
- Bao, X. M. *et al.* Atorvastatin inhibits homocysteine-induced oxidative stress and apoptosis in endothelial progenitor cells involving Nox4 and p38MAPK. *Atherosclerosis.* **210**, 114–121 (2010).
- Changchien, J. J. *et al.* Quinacrine induces apoptosis in human leukemia K562 cells via p38 MAPK-elicited BCL2 down-regulation and suppression of ERK/c-Jun-mediated BCL2L1 expression. *Toxicol Appl Pharmacol.* **284**, 33–41 (2015).
- Hagiwara, S., McClelland, A. & Kantharidis, P. MicroRNA in diabetic nephropathy: renin angiotensin, aGE/RAGE, and oxidative stress pathway. *J Diabetes Res.* **2013**, 392–400 (2013).
- Zampetaki, A. *et al.* Plasma microRNA profiling reveals loss of endothelial miR-126 and other microRNAs in type 2 diabetes. *Circ Res.* **107**, 810–817 (2010).
- Zhang, X. *et al.* MicroRNA-21 modulates the levels of reactive oxygen species by targeting SOD3 and TNF $\alpha$ . *Cancer Res.* **72**, 4707–4713 (2012).
- Wu, X. *et al.* Advanced glycation end products activate the miRNA/RhoA/ROCK2 pathway in endothelial cells. *Microcirculation.* **21**, 178–186 (2014).
- Pan, Y. *et al.* Platelet-secreted microRNA-223 promotes endothelial cell apoptosis induced by advanced glycation end products via targeting the fibroblast-like growth factor 1 receptor. *J Immunol.* **192**, 437–446 (2014).

34. Park, S. Y. *et al.* Synergistic efficacy of concurrent treatment with cilostazol and probucol on the suppression of reactive oxygen species and inflammatory markers in cultured human coronary artery endothelial cells. *Korean J Physiol Pharmacol.* **12**, 165–170 (2008).
35. Biggar, K. K., Kornfeld, S. F. & Storey, K. B. Amplification and sequencing of mature microRNAs in uncharacterized animal models using stem–loop reverse transcription–polymerase chain reaction [J]. *Anal Biochem.* **416**, 231–233 (2011).
36. Xu, Y. *et al.* MicroRNA-335 acts as a metastasis suppressor in gastric cancer by targeting Bcl-w and specificity protein 1. *Oncogen.* **31**, 1398–1407 (2012).

### Acknowledgements

This study was supported by the National Natural Science Foundation (81370883) and the project of Shengjing hospital (MD53).

### Author Contributions

Z.W. and H.L. wrote the main manuscript text, Z.W. and H.L. prepared Figures 1 and 2, H.L. and R.G. prepared Figures 3, 4 and 5, Q.W. prepared Figures 6 and D.Z. prepared figure 7. All authors reviewed the manuscript.

### Additional Information

**Competing financial interests:** The authors declare no competing financial interests.

**How to cite this article:** Wang, Z. *et al.* Antioxidants inhibit advanced glycosylation end-product-induced apoptosis by downregulation of miR-223 in human adipose tissue-derived stem cells. *Sci. Rep.* **6**, 23021; doi: 10.1038/srep23021 (2016).



This work is licensed under a Creative Commons Attribution 4.0 International License. The images or other third party material in this article are included in the article's Creative Commons license, unless indicated otherwise in the credit line; if the material is not included under the Creative Commons license, users will need to obtain permission from the license holder to reproduce the material. To view a copy of this license, visit <http://creativecommons.org/licenses/by/4.0/>